Effect of Tube Support on the Failure of Steam Generator Tubes with Through-Wall Circumferential Cracks

Xin Wang[1], Wolf Reinhardt[2] and Nick Idvorian[2]
[1] Department of Mechanical and Aerospace Engineering, Carleton University, Ottawa, Ontario, Canada, K1S 5B6
[2] Nuclear Engineering, Babcock & Wilcox Canada, Cambridge, Ontario, Canada, N1R 5V3

ABSTRACT

The assessment of steam generator tubes with defects is of great importance for the life extension of steam generators. Circumferential through-wall cracks are the most severe of all tube circumferential defects, and usually require plugging of the affected tubes. The assessment of the tubes with through-wall circumferential cracks or cracks projected to become through-wall can be conducted using the failure assessment diagram (FAD) approach. This approach requires the calculation of the stress intensity factor and the limit load. The available stress intensity factor and limit load solutions for cracked tubes do not include the constraining effect of the tube supports. In the present paper, it is shown that this can be overly conservative. Solutions for stress intensity factors and limit loads are presented for tubes with circumferential through-wall cracks including the effect from the tube support plates. Different values of support spacing are considered. Based on these solutions, the assessment of a typical steam generator tube is demonstrated.

1. INTRODUCTION

The assessment of steam generator tubes with defects is of great importance for the life extension of the nuclear steam generators. Circumferential through-wall cracks are the most severe defects of all tube circumferential indications, and usually they directly result in the plugging of the tubes. If it is suspected that a detected crack might become through-wall before the next plant outage, it is critical that the safe operation of this tube can be demonstrated (safety against rupture). The U.S. Nuclear Regulatory Commission (NRC) requires an evaluation of all detected defects for the affected steam generator tubes to remain in service [1].

The assessment of the tubes with through-wall circumferential cracks can be conducted using the failure assessment diagram (FAD) approach [2, 3]. The knowledge of the stress intensity factor and the limit load for the tubes with the appropriate boundary conditions are necessary to perform a FAD analysis.

The tube axial load under both normal service and accident conditions controls the failure of steam generator tubes with circumferential cracks. Figure 1(a) and 1(b) demonstrate the models used for the cracked tubes under axial load with and without support plates. It can be seen that under an axial tensile stress, rotation at the ends will occur due to the unsymmetrical partial circumferential crack. However, because of the existence of the tube supports, the rotations at the ends are constrainted. This constraint will result in a compressive bending stress at the crack tip. This bending stress effect will help the tube to sustain a larger size crack compared to an unsupported tube. Experimental results showing this effect have been documented by EPRI [4].

The available stress intensity factor and limit load solutions for cracked tubes do not include the effect of the tube supports (as Figure 1(b)). The direct use of those solutions will result in overly conservative failure predictions. In the present paper, stress intensity factors and limit loads are presented for a tube with a circumferential through-wall crack including the restraint from the tube support plates. Different values of spacing of the support are considered. The crack is assumed to be located at mid-span. This is conservative because it minimizes the constraint that the support plates exercise. Based on the obtained solutions, the assessment of a typical steam generator tube with through-wall partial circumferential cracks supported by support plates is demonstrated.

2. STRESS INTENSITY FACTOR SOLUTION

In order to include the effect of the bending constraint into the stress intensity factor, for a given crack size and a tensile stress σ_t, the corresponding bending stress is calculated first. Then the stress intensity factor can be obtained using superposition of the tensile and bending load cases. The bending stress can be calculated by a compliance analysis for the cracked tube. This method was documented by Marchand *et al.* [5] using the example of an edge cracked plate. It is applied to a tube with a single through-wall circumferential crack in the present analysis.

Compliance Analysis Method

For the cracked tube with support plate modeled as shown in Figure 1(a), the reaction bending moment can be calculated by a compliance analysis method as summarized by Marchand *et al.* [5]. For the cracked tube shown in Figure 2, the axial displacement δ and rotation θ of the tube at the support location can be obtained from the summation of "cracked" and "uncracked" components:

$$\begin{pmatrix} \delta_{total} \\ \theta_{total} \end{pmatrix} = \begin{pmatrix} \delta_c \\ \theta_c \end{pmatrix} + \begin{pmatrix} \delta_{nc} \\ \theta_{nc} \end{pmatrix} \tag{2.1}$$

where the index "*c*" relates to the contribution of the crack, and "*nc*" denotes the tube without crack. The compliance relating the force and displacement of the uncracked tube has the standard solution:

$$\begin{pmatrix} \delta_{nc} \\ \theta_{nc} \end{pmatrix} = \begin{bmatrix} L/EA & 0 \\ 0 & L/EI \end{bmatrix} \begin{pmatrix} N \\ M \end{pmatrix} \tag{2.2}$$

In eq. (2.2), N stands for the axial tube force and M for the bending moment. The compliance for the crack is obtained by considering the complementary energy of the specimen, U, in terms of N and M:

$$U(N,M) = \frac{1}{2}\begin{bmatrix} N & M \end{bmatrix} \left(\begin{bmatrix} \delta_c \\ \theta_c \end{bmatrix} + \begin{bmatrix} \delta_{nc} \\ \theta_{nc} \end{bmatrix} \right) \tag{2.3}$$

If we introduce a crack extension dα (see Figure 2), we have

$$\frac{\partial U}{\partial \alpha} = \frac{1}{2}\begin{bmatrix} N & M \end{bmatrix} \begin{pmatrix} \frac{\partial \delta_c}{\partial \alpha} \\ \frac{\partial \theta_c}{\partial \alpha} \end{pmatrix} \tag{2.4}$$

On the other hand, from the relation between stress intensity factor and strain energy release rate under plane stress condition follows that

$$\frac{1}{R_m}\frac{\partial U}{\partial \alpha} = \frac{K_I^2}{E} \tag{2.5}$$

Here K_I is the stress intensity factor solution for the problem shown in Figure 2 and R_m is the mean radius of the tube. The K_I solution is available from Anderson [6], and reprinted in Appendix A of the present paper. It can be written in matrix form as follows:

$$K_I = \begin{bmatrix} \frac{\partial K}{\partial N} & \frac{\partial K}{\partial M} \end{bmatrix} \begin{pmatrix} N \\ M \end{pmatrix} \tag{2.6}$$

The energy change, Eq. (2.5) can be rewritten as

$$\frac{\partial U}{\partial \alpha} = \frac{R_m}{E}\begin{bmatrix} N & M \end{bmatrix} \begin{bmatrix} \left(\frac{\partial K}{\partial N}\right)^2 & \left(\frac{\partial K}{\partial N}\right)\left(\frac{\partial K}{\partial M}\right) \\ \left(\frac{\partial K}{\partial N}\right)\left(\frac{\partial K}{\partial M}\right) & \left(\frac{\partial K}{\partial M}\right)^2 \end{bmatrix} \begin{pmatrix} N \\ M \end{pmatrix} \tag{2.7}$$

Comparing Eqs. (2.4) and (2.7) gives

$$\begin{pmatrix} \frac{\partial \delta_c}{\partial \alpha} \\ \frac{\partial \theta_c}{\partial \alpha} \end{pmatrix} = \frac{2R_m}{E} \begin{bmatrix} \left(\frac{\partial K}{\partial N}\right)^2 & \left(\frac{\partial K}{\partial N}\right)\left(\frac{\partial K}{\partial M}\right) \\ \left(\frac{\partial K}{\partial N}\right)\left(\frac{\partial K}{\partial M}\right) & \left(\frac{\partial K}{\partial M}\right)^2 \end{bmatrix} \begin{pmatrix} N \\ M \end{pmatrix} \tag{2.8}$$

Now integrating with respect to α gives

$$\begin{pmatrix} \delta_c \\ \theta_c \end{pmatrix} = \begin{bmatrix} \int_0^\alpha \frac{2R_m}{E}\left(\frac{\partial K}{\partial N}\right)^2 d\alpha & \int_0^\alpha \frac{2R_m}{E}\left(\frac{\partial K}{\partial N}\right)\left(\frac{\partial K}{\partial M}\right) d\alpha \\ \int_0^\alpha \frac{2R_m}{E}\left(\frac{\partial K}{\partial N}\right)\left(\frac{\partial K}{\partial M}\right) d\alpha & \int_0^\alpha \frac{2R_m}{E}\left(\frac{\partial K}{\partial M}\right)^2 d\alpha \end{bmatrix} \begin{pmatrix} N \\ M \end{pmatrix} \tag{2.9}$$

or

$$\begin{pmatrix}\delta_c\\ \theta_c\end{pmatrix}=\begin{bmatrix}C_{11} & C_{12}\\ C_{21} & C_{22}\end{bmatrix}\begin{pmatrix}N\\ M\end{pmatrix} \tag{2.10}$$

Combining Eq. (2.1), (2.2) and (2.10), the total displacement and rotation are

$$\begin{pmatrix}\delta_{total}\\ \theta_{total}\end{pmatrix}=\begin{bmatrix}L/EA & 0\\ 0 & L/EI\end{bmatrix}\begin{pmatrix}N\\ M\end{pmatrix}+\begin{bmatrix}C_{11} & C_{12}\\ C_{21} & C_{22}\end{bmatrix}\begin{pmatrix}N\\ M\end{pmatrix} \tag{2.11}$$

Eq. (2.11) gives the relationship of the external force and moment to the displacement δ and rotation θ at the support of the cracked tube.

For a given circumferential crack geometry, and given tube axial tensile stress (or tensile force N), the reaction bending moment M can be calculated based on the compatibility condition at the supports.

Effect of the Support Plates

In the real steam generators, support plates support the tube at regular intervals. Each support plate can be thought of as a simple support of the beam that represents the cracked tube. That is, the support restricts the transverse displacement but not the rotation of the tube. A rotational constraint on the tube is created due to the presence of several supports. For convenience, the effect of the rotational constraint on the cracked span can be modeled using a cantilever beam with zero rotation at its end as in Figure 1. If the span of the periodically located supports is L_{real}, then the L (equivalent length of the cantilever) that must be used for zero rotation at the end is found using the method of Appendix B. The equivalent beam length L used in the zero rotation model is found to be

$$L = 1.58L_{real} \tag{2.12}$$

Appendix B gives details of the derivation.

Bending Stress in the Tubes

For a given tube area A, and tensile tube stress σ_t, the corresponding tensile force N is calculated from:

$$N = A\sigma_t \tag{2.13}$$

Then the bending moment M can be obtained by imposing the zero rotation condition at the support plate by applying eq. (2.11). In eq. (2.11), the axial tube force generates a crack opening moment through C_{21}. The support moment is determined by the compliances of tube and crack, and counteracts the opening moment. Note that the C_{11}, C_{12}, C_{21}, C_{22} are calculated from Eq. (2.9). The resulting bending moment is then used to calculate the bending stress σ_b.

$$\sigma_b = \frac{MR}{I} \tag{2.14}$$

The above analysis was conducted using Mathcad [7] for a range of crack dimensions. The typical dimensions used for the tube are:

Tube Outer Diameter: $2R = 0.625$ in
Tube Wall Thickness: $t = 0.038$ in

Three different values of support plate span are considered:

Length of the support plate span: $L_{real} = 22.15, 31.65, 44.30$ in
Equivalent support span $L = 35.0, 50.0, 70.0$ in

The tube material is SB-163 UNS N06690. The material properties are taken from Ref. 2 and 10.

Elastic Modulus: $E = 30.6 \cdot 10^6$ psi
Poisson's Ratio: $\nu = 0.289$

For three different tube support spans, the resulting ratio between the tensile stress σ_t and bending stress σ_b for different angular crack lengths α is obtained and plotted in Figure 3. From these curves, for a given support span value and crack size, the bending stress for any level of tensile stress can be calculated. The resulting tensile stress σ_t and bending stress σ_b can be substituted into eq. (2.6) to calculate the stress intensity factor for tubes with support plate of corresponding span.

3. LIMIT LOAD SOLUTION

In this section, the limit load solutions for tubes with a circumferential through-wall crack are discussed. Analytical solutions for tubes without tube support and finite element solutions for tubes with tube support are presented.

Analytical Limit Load Solutions

Two limiting assumptions can be made about the failure of the cracked tube, namely either that it fails purely due to membrane stress, or that it fails only due to bending. These two limiting assumptions can be combined to give a lower bound limit load.

The limit load for the case where failure occurs due to membrane stress depends linearly on the degraded area through

$$\frac{F_{ax}}{\sigma_f A_0} = 1 - \beta \tag{3.1}$$

and

$$\beta = \frac{A_{crack}}{A_0} = \frac{\alpha}{\pi} \tag{3.2}$$

where F_{ax} is the limit axial force, σ_f is the flow stress and A_0 is the cross sectional area of the uncracked tube. The cracked area A_{crack} is proportional to the angular length of the crack, α (Figure 2). The fraction of degraded area is denoted by β. The percentage of β is also called PDA (percentage degraded area). Failure in membrane of the present crack could occur if the tube is restrained such that no rotation of the tube can occur at the crack location (rigidly held tube).

For the second limiting case, the membrane contribution to failure is neglected, and collapse by pure bending is assumed. A bending moment is caused by the unsymmetrical location of the crack, which moves the neutral axis towards the uncracked side of the tube. The amount x_s by which the neutral axis moves at the cracked section can be found to be

$$x_s = \frac{2}{3}\frac{r_o^2 + r_o r_i + r_i^2}{r_o + r_i}\frac{\sin\alpha}{\pi - \alpha} \tag{3.3}$$

where $r_o = R$ is the outer and r_i is the inner radius of the tube. The moment generated by the applied axial force is $M_{app} = F_{ax}$ x_s. At the limit state, this moment equals the plastic hinge moment. The resulting equation can be solved for the dimensionless axial force at collapse to give

$$\frac{F_{ax}}{\sigma_f A_o} = \frac{4}{3}\frac{\sqrt{(r_o^2 - x_s^2)^3} - \left\langle \sqrt{(r_i^2 - x_s^2)^3} \right\rangle}{x_s A_o} - \frac{A_m}{A_o} \tag{3.4}$$

and

$$A_m = \frac{\pi}{2}\left[r_o^2 - \langle r_i^2 \rangle\right] - \left[r_o^2 \arcsin\frac{x_s}{r_o} - \left\langle r_i^2 \arcsin\frac{x_s}{r_i} \right\rangle\right] \tag{3.5}$$

where the contents of the $\langle\ \rangle$ brackets is zero if $x_s > r_i$. For short cracks when α is small, (3.4) gives a higher limit load than (3.1) because the moment arm x_s is small. On the other hand, above a PDA of about 30%, the bending case becomes the more restrictive one. However, for this failure mode to prevail, the tube must be completely free to rotate (unrestrained) to allow the cracked area a limit failure in bending.

An expression for the lower bound limit load for a combined membrane and bending failure of an unrestrained tube is given by Anderson [6]. Solved for the dimensionless axial force $F_{ax}/(\sigma_f A_0)$, the lower bound limit load is

$$\frac{F_{ax}}{\sigma_f A_0} = 1 - \frac{\alpha}{\pi} - \frac{2}{\pi}\arcsin\left(\frac{1}{2}\sin\alpha\right) \tag{3.6}$$

This formula describes the plastic collapse of a tube that is completely unrestrained against rotations. The failure mode of this tube is combined membrane and bending (as opposed to (3.4) which describes only the bending contribution). The limit loads from (3.1), (3.4) and (3.6) are compared in Fig. 4. It can be seen how the lower bound formula (3.6) bounds both (3.1) and (3.4), and how the membrane mode and the bending mode dominate for lower and higher PDA, respectively.

Finite Element Solution

The finite element method is used to calculate the limit load for a supported tube. A three-dimensional finite element model (ANSYS, [8]) of a half tube was created using 8-noded shell elements. The same tube dimensions as in Section 2 are used. Note that elastic – perfectly plastic properties have been assumed with a flow stress of 55.75 ksi.

The crack was modeled by deleting a row of elements at one end of the model up to the desired angular location. The model is shown in Fig. 5.

The model has symmetry displacement boundary conditions applied on the axial section surface and on the crack ligament (cross sectional) surface. The cross sectional surface at the other end of the tube is restrained against radial and circumferential displacements. The nodes are coupled to prevent any bending deflection of the tube, but to allow axial displacements. The uniformly distributed axial end force is applied to the same surface. The boundary conditions are

indicated in Fig. 5. The boundary conditions represent two pieces of catilevered tube of span 35, 50, 75 inch length each with a mid-span crack.

The finite element model described here was analyzed with a PDA of 10% to 90% in steps of 10%. Due to very high strains in the element at the "crack tip", convergence problems were occasionally encountered, and the convergence tolerance for the force was increased to 1.5% in some runs. Therefore, the limit load results do not all fall on a smooth curve.

The results are depicted in Fig. 6. As expected, the results lie between the limiting curves (3.1) and (3.6). For cracks up to 30% PDA, the limit load follows (3.6) fairly closely, while for larger PDA, the limit load approaches the membrane failure curve (3.1). Note that detailed finite element analysis indicates that the results for three different spans (35, 50 and 75 in) are within 1% to each other, therefore, only the results for 50 in span is plotted and it is applicable for any span range from 35 to 70 in.

This new curve will be used as the limit load solution for the cracked tubes with tube support plates in the next section.

4. FAILURE ASSESSMENT OF CRACKED TUBE

Based on the stress intensity factor solutions and limit load solutions presented in Section 2 and 3, the failure assessment of circumferential cracked tube with tube support is conducted. In the present analysis, the failure assessment diagram approach of Level 3 of PD6493 is used [9]. Note that only the assessment for a through-wall circumferential crack in the SG tube with tube support span value of 50 in. is conducted here. The assessments for other tube span values can be conducted similarly with the results obtained in section 3.

The assessment of the potential of failure is determined by the distance from the origin of the failure assessment diagram (FAD) to the calculated assessment point (K_r, L_r) determined from

$$K_r = \frac{K_I}{K_{IC}} \tag{4.1}$$

and

$$L_r = \frac{\sigma}{\sigma_L} \tag{4.2}$$

divided by the distance from the origin to the failure assessment curve. Note that K_r is the stress intensity ratio with K_I being the stress intensity factor for the crack and K_{IC} the toughness of the material. The parameter L_r is the stress ratio, which is the ratio of the applied stress to the limit stress solution calculated based on the yield stress.

In PD6493 [9], a lower bound FAD curve that is independent of geometry and the material stress-strain curve is given by:

$$K_r = (1 - 0.14L_r^2)\left[0.3 + 0.7\exp(-0.65L_r^6)\right] \tag{4.3}$$

Since the load ratio is defined in terms of the yield strength, L_r can be great than 1. The typical cut-off is 1.2 for C-Mn Steel and 1.8 for austentic stainless steel [9]. Since the Alloy 690 is an austentic material, the cut-off of 1.8 is used. Figure 7 shows a plot of the failure assessment diagram.

For the assessment, a range of stresses is applied which corresponds to different operating conditions of the steam generator. The maximum crack size for each loading condition, represented by PDA (percentage degraded area), is obtained from the failure assessment diagram. The axial stress is normalized as follows:

$$P_n = \frac{\sigma}{\sigma_f} \tag{4.4}$$

where σ_f is the flow stress of the material equals $0.5(\sigma_y + \sigma_u)$, with σ_y and σ_u yield and ultimate strengths, respectively. The yield strength and ultimate strength of Alloy 690 are taken at 650 deg. F, where they equal 31.5 ksi and 80 ksi, respectively [2, 10]. The fracture toughness K_{IC} is obtained by converting a conservative J_{IC} value. The J_{IC} value used is 571 in-lb/in^2 based on a conservative estimation.

The resulting maximum PDAs for a normalized axial stress are presented in Figure 8. As a comparison, the PDA results for tubes without tube support are also shown. It can be observed that it is overly conservative to exclude the effect of the tube supports. By accounting for the effect of the tube support plates, the increase in the allowable PDA can be as much as 15% in the present example.

5. CONCLUSIONS

The stress intensity factors and limit loads are presented for tubes with circumferential through-wall cracks when taking the restraining effect of the tube support plates into account. Based on the presented solutions, the assessment of

typical steam generator tube with through-wall circumferential cracks of various sizes is conducted. It is demonstrated that the maximum allowable PDA can increase by as much as 15% compared to an assessment that does not consider the restraint of the tube support plates.

REFERENCES

1. NRC Regulatory Guide 1.121, August, 1976, "Bases for Plugging Degraded PWD Steam Generator Tubes", U.S. Nuclear Regulatory Commission.
2. ASME Boiler & Pressure Vessel Code, 1998 Edition, Section III and XI, including Appendices.
3. J. Bloom, 1985, "Deformation Plasticity Failure Assessment Diagram", Elastic-Plastic Fracture Mechanics Technology", ASTM STP 896.
4. EPRI TR-107197-P1 & P2, Interim Report, November 1997, "Depth-Based Structural Analysis Methods for Steam Generator Circumferential Indications".
5. Marchand, N., Parks, D.M. and Pelloux, R.M. , 1986, "K_I Solutions for Single Edge Notch Specimens under Fixed End Displacement", International Journal of Fracture, Vol. 31, pp. 53 – 65.
6. Anderson, T.L., 1995, Fracture Mechanics, Fundamentals and Applications, Second Edition, CRC Press Inc., Boca Raton.
7. Mathcad 6.0, 1995, User's Manual, MatSoft Inc.
8. ANSYS Release 5.6, 1999, User's Manual, 11th Edition, ANSYS Inc.
9. PD 6493:1991, August 1991, "Guidance on Some Methods for the Derivation of Acceptance Levels for Defects in Fusion Welded Joints", British Standards Institution.
10. Huntington Alloys, 1980, "Inconel Alloy 690", Huntington Alloys, Inc.
11. Young, W.C., 1989, "Roark's Formulas for Stress and Strain", 6th Edition, McGraw-Hill Inc., New York.

APPENDICES

A: Stress Intensity Factor Solutions for Partial Through-Wall Circumferential Cracks

From Anderson [6] the stress intensity factor for problem described in Figure 2 is written as

$$K_I = \begin{bmatrix} \frac{\partial K}{\partial N} & \frac{\partial K}{\partial M} \end{bmatrix} \begin{pmatrix} N \\ M \end{pmatrix}$$

where

$$\frac{\partial K}{\partial N} = \left[1 + A \left[5.3303 \cdot \left(\frac{\alpha}{\pi} \right)^{1.5} + 18.773 \cdot \left(\frac{\alpha}{\pi} \right)^{4.24} \right] \right] \cdot \frac{\sqrt{\pi R \alpha}}{2\pi R t}$$

$$\frac{\partial K}{\partial M} = \left[1 + A \left[4.5967 \cdot \left(\frac{\alpha}{\pi} \right)^{1.5} + 2.6422 \cdot \left(\frac{\alpha}{\pi} \right)^{4.24} \right] \right] \cdot \frac{\sqrt{\pi R \alpha}}{R^2 t}$$

and $$A = \left(0.125 \cdot \frac{R}{t} - 0.25 \right)^{0.25} \text{ for } 5 \le \frac{R}{t} \le 10$$

B: Derivation of a Cantilever Beam Length Equivalent in Stiffness to an Infinite Periodically Supported Tube

Consider a semi-infinite beam with evenly spaced (distance L_{real}) supports, ending in a cantilever of $L_{real}/2$ as shown in the figure below.

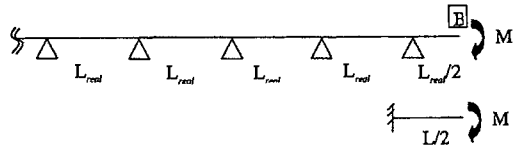

Figure B.1: Periodically Supported Beam and Equivalent Cantilever

The objective is to find the equivalent length L of a simple cantilever beam such that an applied moment M causes the same rotation θ as at the end point B of the semi-infinite beam.

First, consider a cantilevered beam of length $L_{real}/2$ with simple support and a torsional spring of stiffness C_0 at one end. Given the moment of area I and the Young's modulus E, the end rotation θ is [11]:

$$\theta\left(\frac{L_{real}}{2}\right) = \frac{ML_{real}}{2EI} + \frac{M}{C_0} \tag{B1}$$

The rotational stiffness C_0 is caused by the semi-infinite simply supported beam that is loaded by a moment on the last support. In this situation, a single simply supported beam of length L_{real} has the stiffness [11]:

$$C_{B1} = \frac{3EI}{L_{real}} \tag{B2}$$

If this single beam is attached to another identical beam, the next beam imposes a moment on the other end of the beam, and the effective stiffness increases. The same is true if another beam is added to this structure, and so on. The rotational stiffness of an n-beam structure can be expressed in terms of the stiffness of the n-1 beam structure that is attached to a single simply supported beam through

$$C_{Bn} = C_{B1}\frac{1+\dfrac{C_{Bn-1}}{C_{B1}}}{1+\dfrac{3}{4}\dfrac{C_{Bn-1}}{C_{B1}}} \tag{B3}$$

This recursion formula converges quickly to a stationary value that is assumed when $n \to \infty$. By using the condition $C_{B\,n} = C_{B\,n-1}$ in (B3), it can be shown that

$$C_{B\infty} = \frac{2\sqrt{3}}{3}C_{B1} \tag{B4}$$

Going back to the initial cantilever portion of the infinite beam, one can now substitute $C_0 = C_{B\infty}$ into (B1) to obtain

$$\theta\left(\frac{L_{real}}{2}\right) = \frac{ML_{real}}{2EI}\left(1+\frac{\sqrt{3}}{3}\right) \tag{B5}$$

Now using the simple cantilever beam with length L, the required equivalent length L is found to be

$$L = L_{real}\left(1+\frac{\sqrt{3}}{3}\right) = 1.58L_{real} \tag{B6}$$

Therefore, the required length L in the model is $1.58L_{real}$.

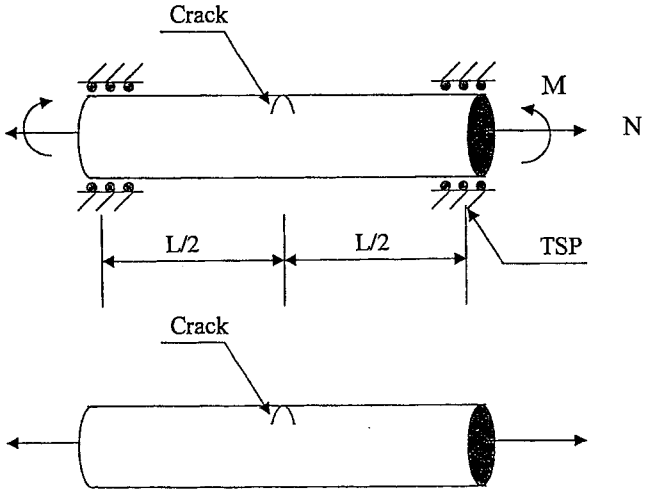

Figure 1 Tubes with and without Tube Support Plates
(a): with Tube Support Plates, (b): without Tube Support Plates.

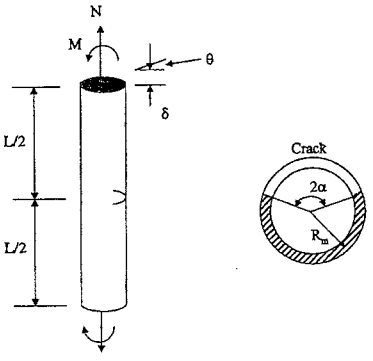

Figure 2. Analysis of Displacement and Rotation

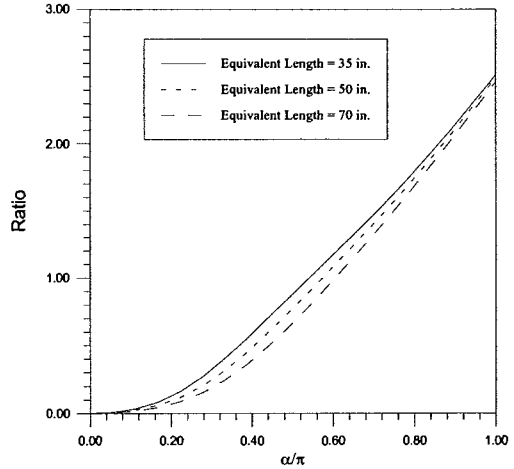

Figure 3. Crack Length vs. Bending Stress σ_b to Tensile Stress σ_t Ratio (σ_b/σ_t)

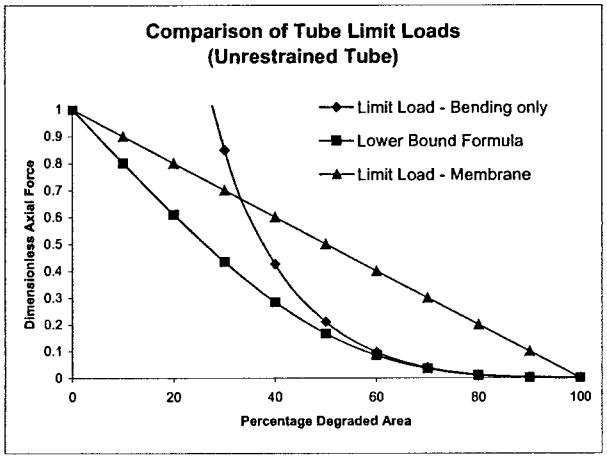

Figure 4. Comparison of Tube Limit Loads (Unrestrained Tubes)

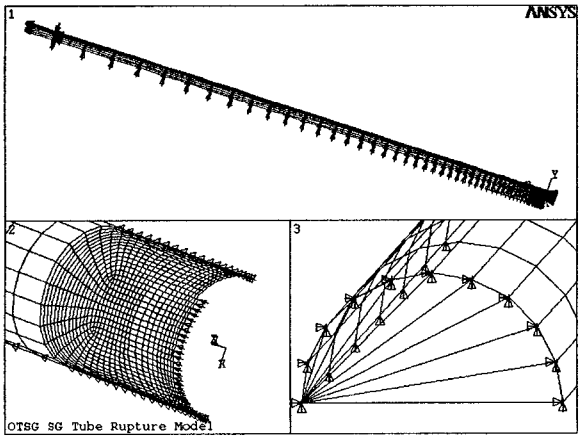

Figure 5. The Finite Element Model of the Tube with Tube Support

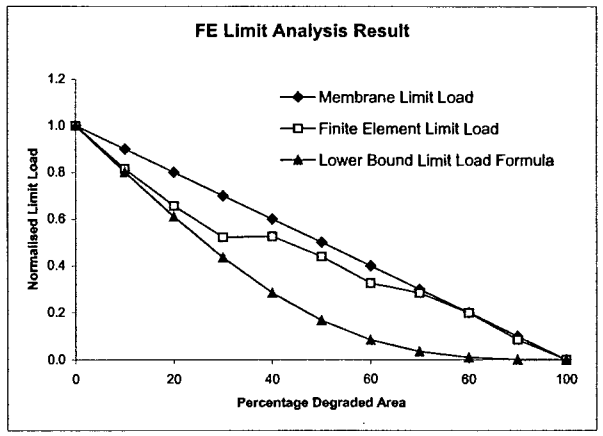

Figure 6. Finite Element Limit Load Analysis Results

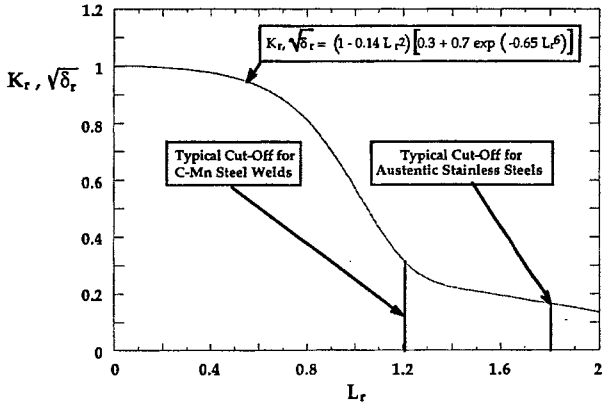

Figure 7. Failure Assessment Diagram Level 3 of PD: 6493 (BSI, 1991)

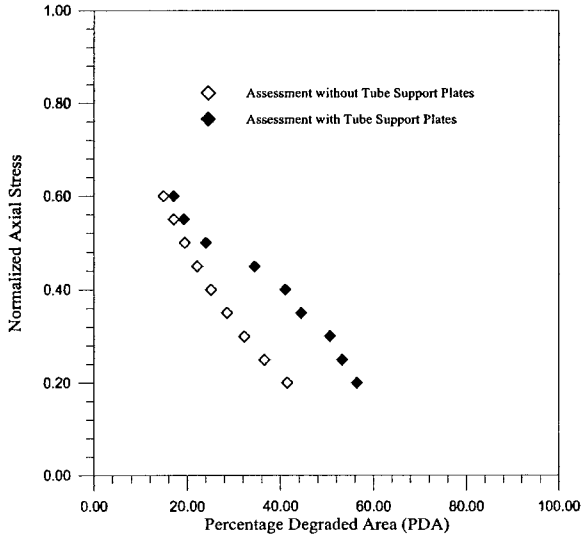

Figure 8 Results from the Failure Assessment